Determinate arbitrary quantum state engineering through one-dimensional quantum walks

Yu Wang [1,*] Meng Li [2,†] and Yuan-Yuan Zhao [3,‡]

[1] Beijing Institute of Mathematical Sciences and Applications (BIMSA), Beijing 101408, China
[2] State Key Lab of Processors, Institute of Computing Technology, Chinese Academy of Sciences, Beijing 100190, China
[3] Quantum Science Center of Guangdong-Hong Kong-Macao Greater Bay Area (Guangdong), Shenzhen 518045, China

(Received 31 October 2024; accepted 29 May 2025; published 11 June 2025)

Efficient generation of arbitrary superposed quantum states in high-dimensional systems is crucial for various quantum technologies but remains fundamentally challenging because of the intricate and extensive parameter control. In this work, we propose a generalized discrete one-dimensional quantum walk model with time- and position-dependent coin operations, and varied shift lengths. This approach enables deterministic and direct preparation of any qudit state $|\phi\rangle = \sum_{k=0}^{d-1} a_k|k\rangle$ using binary or ternary tree structures, without solving quadratic equations. Our method requires only $O(\log d)$ steps and $O(d)$ coin operations, significantly reducing the resource requirements compared to the previous approach of $O(d)$ steps and $O(d^2)$ coin operations. Additionally, we propose an experimental scheme based on successive interferometers, demonstrating that our method is compatible with current state-of-the-art experimental technologies. This efficient method for preparing quantum superposition states lays a foundation for advancing quantum technologies, with broad applications in quantum information processing.

DOI: 10.1103/2frm-2v6m

I. INTRODUCTION

Quantum superposition is a fundamental principle of quantum mechanics and an important resource of quantum information processing [1]. While a superposed qubit (two-dimensional system) is often the carrier of quantum communication and computation tasks, a qudit (d-dimensional system) allows for a larger state space to store and process information. Therefore, qudits have attracted additional research interest owing to their superior potential in fundamental tests of quantum mechanics, quantum communication protocols, universal quantum computations, and initial input of quantum algorithms [2–6].

For two-dimensional encoding systems, such as the commonly used polarization degree of freedom in photonic platforms or spin-1/2 systems, qudit state preparation often involves entanglement between different particles. In cases where $d = 2^n$, various approaches have been explored using the circuit model. While efficient protocols exist for specific subsets of qudits, preparing arbitrary superpositions of n qubits requires a general engineering algorithm that incurs a cost of at least $O(2^n/\log n)$ gates [7]. The circuit depth can be reduced to $O(n^2)$ by using an exponential number of ancillary qubits [9]. These factors pose challenges for the accuracy and scalability of NISQ devices. Significant efforts have been made to minimize gate counts [8,10,11], optimize circuit depth [12,13], introduce ancillary qubits [14,15], and prepare sparse states [9,16,17]. Additionally, methods for probabilistically preparing qudits using variational quantum circuits have been proposed [18–20], although issues like barren plateaus can limit the preparation of arbitrary qudits [21,22].

There are numerous systems that naturally support high-dimensional encodings, such as the path, time-bin, and OAM degrees of freedom of photons [23]. Engineering such systems into qudit states eliminates the need for complex entangling operations between particles. However, efficiently driving a high-dimensional system into an arbitrary superposed qudit state, $|0\rangle \to |\phi\rangle = \sum_{k=0}^{d-1} a_k|k\rangle$, where $\sum_k |a_k|^2 = 1$, remains a significant challenge [24]. The large number of parameters required to describe these states and operations demands precise control of the protocols. Despite successful qudit state preparation across various physical platforms [25–32], the specific dynamics of each system make it difficult to develop universal translation methods for qudit preparation.

In this work, we explore qudit state preparation using quantum walk models. Quantum walks (QWs), the quantum analogs of classical random walks [33], have proven to be powerful tools for engineering particle states in large Hilbert spaces via coin operators. The one-dimensional (1D) discrete QW model [34], the simplest form of QW, involves a walker whose position evolves based on coin tosses. Early studies on QWs with fixed shift length focused on their unique behavior, distinct from classical random walks, and employed various types of coin operations, including unbiased [35], time-dependent [36–38], position-dependent [39–41], history-dependent [42,43], and randomly chosen coins from a set [44–46]. Extending the QW model to include variable shift lengths enables hyper-ballistic diffusion [47,48]. We employ a general one-dimensional quantum walk model, incorporating

*Contact athor: wangyu@bimsa.cn
†Contact athor: limeng2021@ict.ac.cn
‡Contact athor: zhaoyuanyuan1@quantumsc.cn

Published by the American Physical Society under the terms of the Creative Commons Attribution 4.0 International license. Further distribution of this work must maintain attribution to the author(s) and the published article's title, journal citation, and DOI.

time- and position-dependent coin operations and variable shift lengths, to address the problem of quantum state engineering.

Note that creating superpositions of the high-dimensional system in fact corresponds to efficiently achieving a probability distribution among the basis [49]. Thus, the problem of qudit preparation can be viewed as an inverse problem compared to previous works—that is, determining the appropriate coin operations needed to achieve a desired target probability distribution [50,51]. Meanwhile, with advancements in quantum technologies, QWs have been experimentally realized across various platforms [52], including photonic systems [53,54], ion traps [55], ultracold atoms [56], and superconducting circuits [57,58]. Therefore, investigating qudit preparation using the QW model is not only theoretically intriguing but also holds significant practical relevance.

Specific qudit states have been prepared using QWs [59–61], as well as qubit-qudit entangled states [46,62]. Additionally, when coin operations are time dependent, it becomes possible to prepare nearly all qudit states with nonzero probability, except for a measure-zero subset [63,64]. This method requires solving $O(d)$ quadratic equations to determine the necessary coin operations and involves a total cost of $O(d^2)$ coin operations. For general multi-qudits, the proposed preparation protocol requires $O(d)$ steps [65]. Two-dimensional quantum walk evolution can also be used as a tool for the generation of high-dimensional qudit states, which only takes $O(\sqrt{d})$ steps [66].

In this work, we introduce a generalized 1D QW model for the deterministic and direct preparation of arbitrary probability distributions and superposed qudit states. In our model, the coin operators at each step are both position and time dependent, and the shift lengths vary with time. Overall, our approach requires only $O(\log d)$ steps of QWs, with the total number of coin operations scaling as $O(d)$. This model presents three improvements over previous qudit preparation methods using 1D QWs [63,64]. First, we directly define the coin operations without the need to solve quadratic equations, reducing the total number of coin operations from $O(d^2)$ to $O(d)$. Second, we can prepare all qudit states without concerns about solvability, as there is no failure set of nonengineerable qudits. Third, by eliminating entanglement in the final state, we increase the success probability from approximately 0.33 to 1. Additionally, the modified shift lengths can be readily implemented in optical systems. We believe this method opens avenues for applying QW to high-dimensional quantum information processing tasks.

II. MODEL OF 1D QWs

We begin by introducing the generalized 1D QW model. Unlike previous types (see details in Appendix A), in the general case, more freedoms can be introduced for the choices of shift lengths in each step. This makes the protocols of probability and qudit generation simple yet efficient.

The entire physical system is characterized by a compound Hilbert space, denoted as $\mathcal{H}_P \otimes \mathcal{H}_C$. Here, $\mathcal{H}_P$ represents the position space in which the walker traverses, spanned by the basis states $\{|n\rangle : n \in \mathbb{Z}\}$. $\mathcal{H}_C$ denotes the coin space that governs the walker's movement, spanned by the basis states $\{|0\rangle, |1\rangle\}$. The complex dynamic of a single-step 1D QW is described with $W = T \cdot (I \otimes C)$, where C is the operation applied on coin space and T is the shift operation, which decides how the walker moves on the position space according to the evolved coin state.

Model A. (1D QW with time- and position-dependent coin operations, bidirectional movement, and variable shift lengths.) The entire dynamic of the general kth QW is given by

$$W_k = T_k \cdot \left[\sum_{j=-\infty}^{+\infty} |j\rangle\langle j| \otimes C(k, j) \right], \tag{1}$$

where $C(k, j)$ is a one-qubit coin operation acting on position j, and

$$T_k = \sum_{n=-\infty}^{+\infty} |n - l_k\rangle\langle n| \otimes |0\rangle\langle 0| + |n + l_k\rangle\langle n| \otimes |1\rangle\langle 1|. \tag{2}$$

Here, l_k denotes the shift length at the kth step. If the coin state is $|0\rangle$, the walker moves from position n to $n - l_k$; if it is $|1\rangle$, the walker moves to $n + l_k$.

Time- and position-dependent 1D QWs have been extensively used, both theoretically and experimentally, to simulate generalized POVMs [67–69], proving their utility across various quantum information tasks. With the addition of a variable shift length, we believe this more general QW model will find applications in a wider range of quantum information processing tasks.

Variable shift lengths provide an additional layer of adaptability, enabling more intricate and versatile simulations of complex quantum behaviors that are difficult to achieve with fixed shift lengths of 1. Moreover, the shift operation with variable lengths can be readily implemented. Firstly, the operation T_k in Eq. (2) can be realized by applying the single-step operation T_1 (with $l_1 = 1$) iteratively l_k times. Thus, any system capable of implementing QWs with length 1 can execute the scheme with the variable shift length discussed in this paper.

Secondly, the implementation of T_k in some systems may be more convenient. In optical systems, particularly those involving orbital angular momentum (OAM), a shift length of ± 1 is realized using a q plate with $q = 1/2$ in qudit generation [63,64]. By adjusting the q value to $l_k/2$, variable shift lengths l_k can be achieved with one q plate, allowing the number of steps (or devices) required for the shift operation to be reduced exponentially.

Then, introducing variable shift lengths not only enriches the theoretical framework of quantum walks but also establishes a concrete path towards practical implementation on optical platforms, bridging the gap between theory and experiment.

Let the initial state be

$$|\Psi\rangle = |0\rangle_p |0\rangle_c. \tag{3}$$

After t steps of a 1D QW, the final state will be

$$|\Psi_t\rangle = W_t \cdots W_2 W_1 |\Psi\rangle. \tag{4}$$

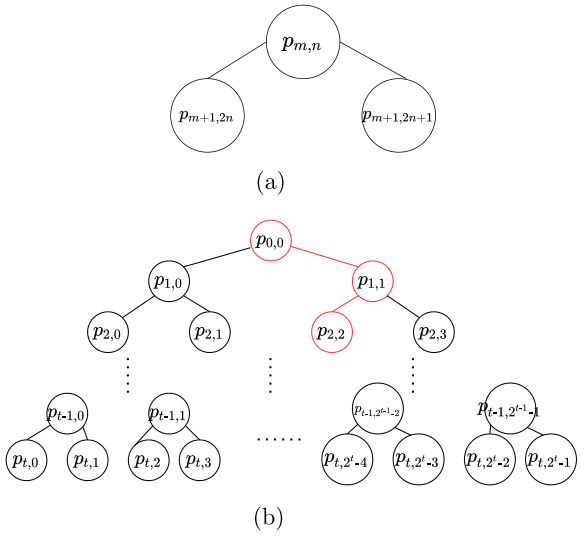


FIG. 1. (a), (b) Subfigures representing the structure of a binary tree. (a) Subtree. Here $m \in \{0, \cdots, t-1\}$ and $n = 0, \cdots, 2^m - 1$. and (b) Illustration of binary tree.

III. ARBITRARY PROBABILITY BY QWs

To simulate an arbitrary probability distribution

$$\{p_0, p_1, \ldots, p_{d-1}\}, \tag{5}$$

we first adjust the distribution to have a size that is a power of two. If d is not a power of two, we append zeros to create a new distribution $\{p_0, p_1, \ldots, p_{d-1}, p_d = 0, \ldots, p_{2^t-1} = 0\}$, where $t = \lceil \log_2 d \rceil$.

Next, we arrange the 2^t probabilities into a binary tree structure to facilitate recursive processing. The leaf nodes of the tree correspond to the probabilities

$$\{p_{t,0}, p_{t,1}, \ldots, p_{t,2^t-1}\}, \tag{6}$$

where $p_{t,j} = p_j$ for $j = 0, 1, \ldots, 2^t - 1$.

Each parent node in the tree is obtained by summing its two child nodes at the next level down. This relationship can be expressed as

$$p_{m,n} = p_{m+1,2n} + p_{m+1,2n+1},$$

where $p_{m,n}$ represents the parent node at level m and index n, while $p_{m+1,2n}$ and $p_{m+1,2n+1}$ are its child nodes at the next level $m+1$, as shown in Fig. 1(a). Figure 1(b) shows the complete binary tree generated iteratively from the probability distribution in Eq. (6), with the root node of the tree being $p_{0,0} = 1$.

The key aspect of our scheme is the design of variable shift lengths and the corresponding time- and position-dependent coin operations at each step.

Shift Lengths. At the kth step of the QW, we set the shift length l_k as

$$l_k = 2^{t-k}, \quad \text{where } k = 1, \ldots, t. \tag{7}$$

Coin operations. The time- and position-dependent coin operations $C(k, j)$ are related to the nodes in the binary tree. For each parent node $p_{m,n}$ in Fig. 1(a), we define a *node unitary operation* $M(m, n)$ as

$$M(m,n) = \frac{1}{\sqrt{p_{m,n}}} \begin{pmatrix} \sqrt{p_{m+1,2n}} & -\sqrt{p_{m+1,2n+1}} \\ \sqrt{p_{m+1,2n+1}} & \sqrt{p_{m+1,2n}} \end{pmatrix}. \tag{8}$$

When $p_{m,n} = 0$, the operation $M(m, n)$ can be arbitrary or saved as I, as the walker will not appear at the corresponding positions.

At the kth step of the QW, the walker can be in at most 2^{k-1} different positions. From the leftmost to the rightmost positions, we sequentially perform coin operations

$$C(k, j) = M(k-1, n) X^n, \tag{9}$$

where $n = 0, 1, \ldots, 2^{k-1} - 1$ and j denotes the position corresponding to index n. Here, $X^n = I$ for even n, and $X^n = X$ for odd n, with X being the Pauli X matrix.

To accurately determine the position j where we apply the coin operation $M(k-1, n)X^n$ at step k, we need to trace the path from the root node $p_{0,0}$ to the leaf node $p_{k-1,n}$ in the binary tree. This path is represented as:

$$p_{0,0} \to p_{1,g(1,k-1,n)} \to \cdots \to p_{k-2,g(k-2,k-1,n)} \to p_{k-1,n},$$

where the nodes along the path are denoted as $p_{h,g(h,k-1,n)}$ with $h = 1, 2, \ldots, k-1$.

The position j is then calculated using the formula

$$j = \sum_{h=1}^{k-1} 2^{t-h} \times (-1)^{g(h,k-1,n)+1}. \tag{10}$$

At the first step of the quantum walk, the walker has not yet moved and remains at the initial position 0 (corresponding to the probability $p_{0,0}$). Therefore, at the kth step with $k \geqslant 1$, the walker has completed $k-1$ rounds of evolution and can be located at 2^{k-1} possible positions, representing all potential destinations after $k-1$ steps.

Each position j is reached from the starting point 0, with a displacement of 2^{t-h} at the hth step ($h = 1, 2, \ldots, k-1$). A factor of -1 is applied for leftward movement, and a factor of 1 for rightward movement, with the direction determined by the parity of $g(h, k-1, n)$. After kth step of QW, the evolved state will be in 2^k different positions. With this design, after the coin operation at the $(k+1)$th step, we obtain the state described in Eq. (B2) in the Appendix.

For example, we consider the p_{22} in Fig. 1(b). The coin operation $M(2, 2)X^2$ will be used as the third step. The position for $M(2, 2)$ is $2^2 - 2^1 = 2$.

Result 1. After performing k steps of the 1D QW in Eq. (1), utilizing the designed shift lengths in Eq. (7) and coin operations in Eq. (9), measuring the position space in the basis states $\{\ldots, |-1\rangle, |0\rangle, |1\rangle, \ldots\}$ yields the probability distribution $\{p_{k,0}, p_{k,1}, \ldots, p_{k,2^k-1}\}$ corresponding to the kth layer of the binary tree.

Furthermore, after t steps, the probability distribution in Eq. (6) will be obtained from the leftmost position $-2^t + 1$ to the rightmost position $2^t - 1$ with interval 2. The details and examples are given in Appendix B 1.

IV. PROBABILITY DISTRIBUTION TO QUDIT GENERATION SCHEME

The arbitrary superposed qudit to prepare is

$$\sum_{k=0}^{d-1} a_k|k\rangle, \quad \text{where} \quad \sum_{k=0}^{d-1} |a_k|^2 = 1. \tag{11}$$

Let $t = \lceil \log_2 d \rceil$. Each complex number a_k is written as $a_k = \sqrt{p_k}e^{i\theta_k}$, where $p_k = |a_k|^2$, $\theta_k \in [0, 2\pi)$.

Result 2. Each probability distribution protocol by QW can be transformed into a specialized qudit preparation protocol by adjusting the coin operators and shift lengths.

Analysis. Suppose that after performing t steps of the 1D QW, we simulate a probability distribution $\{p_0, p_1, \ldots, p_{d-1}\}$ at the positions $\{k_0, k_1, \ldots, k_{d-1}\}$ of the walker. The evolved state is then given by

$$|\Psi_t\rangle = \sum_{l=0}^{d-1} \sqrt{p_l}\,|k_l\rangle \otimes (A_{k_l}|0\rangle + B_{k_l}|1\rangle), \tag{12}$$

where $|A_{k_l}|^2 + |B_{k_l}|^2 = 1$. It closely resembles a generalized qudit at position space, differing only in two aspects: the phases and the coin states.

We introduce an additional $(t+1)$th step. The coin operations $C(t+1, k_l)$ at position $|k_l\rangle$ are designed to transform the state $A_{k_l}|0\rangle + B_{k_l}|1\rangle$ into $e^{i\theta_l}|0\rangle$. Additionally, we set the shift length $l_{t+1} = 0$. After the $(t+1)$th step, the evolved state becomes

$$|\Psi_{t+1}\rangle = \left(\sum_{l=0}^{d-1} \sqrt{p_l}\, e^{i\theta_l}|k_l\rangle\right) \otimes |0\rangle. \tag{13}$$

By applying QW Model B (or C), the target probability distribution over arbitrary positions $\{k_0, k_1, \ldots, k_{d-1}\}$ can be precisely shifted and reindexed to the standardized position set $\{0, 1, \ldots, d-1\}$. This transformation facilitates the preparation of the desired qudit state in the position basis: $\sum_{k=0}^{d-1} \sqrt{p_k}\, e^{i\theta_k}|k\rangle$, where the position basis states are now uniformly spaced. ■

Using this technique with QW Model A, we can obtain the state

$$|\phi\rangle = \sum_{k=0}^{2^t-1} \sqrt{p_k}e^{i\theta_k}|-2^t+1+2k\rangle. \tag{14}$$

This method is referred to as Technique 1, which involves performing an additional d coin operations at the $(t+1)$th step. Furthermore, new method (Technique 2) can be employed to reduce the number of required coin operations by half. This optimization is achieved by modifying the coin operations at the tth step, as half of the coin states is already $|0\rangle$ and the other half is $|1\rangle$. Further details are provided in Appendix B 3.

In the circuit model, Grover and Rudolph presented a simple and efficient method for generating superposed qudits, which can form specific probability distributions [49]. By utilizing 1D QWs with variable shift lengths, these probability distributions can be generated arbitrarily, allowing for the straightforward preparation of all superposed qudit states.

If we change the initial position of walker from $|0\rangle$ to $|2^t - 1\rangle$, the final prepared state will be $|\phi'\rangle = \sum_{m=0}^{2^t-1} a_m|2m\rangle$. However, a two-unit gap still exists between adjacent positions.

V. NEW 1D QW MODELS

To reduce the gap between adjacent positions to one unit, we can adjust the shift directions in Eq. (2) using the new Models B and C. This adjustment allows for a denser distribution of the walker's positions, facilitating more precise control over the qudit state preparation.

Model B. (Single direction with time-dependent and position-dependent coins, varied shift length.)

The walker either remains stationary or moves to the right. The position space $\mathcal{H}_p$ is changed to the one spanned by states $\{|k\rangle : k = 0, 1, \cdots\}$. The shift regulation changes from T into

$$S = \sum_{n\geqslant 0} |n\rangle\langle n| \otimes |0\rangle\langle 0| + |n+1\rangle\langle n| \otimes |1\rangle\langle 1|. \tag{15}$$

If the tossed coin is 0, the walker stands still. If it is 1, the walker steps ahead.

In general, the shift length l_k can be dependent on the time. The shift operation at the kth step is the following:

$$S_k = \sum_{n\geqslant 0} |n\rangle\langle n| \otimes |0\rangle\langle 0| + |n+l_k\rangle\langle n| \otimes |1\rangle\langle 1|. \tag{16}$$

The entire dynamic of the general 1D QW at the kth step is given by

$$V_k = S_k \cdot \left[\sum_{j=0}^{+\infty} |j\rangle\langle j| \otimes C(k, j)\right]. \tag{17}$$

To generate an arbitrary probability distribution, the shift lengths are also set as defined in Eq. (7), and the coin operations are applied as in Eq. (9). However, the positions at which the coin operations are performed are modified from Eq. (10) to

$$j = \sum_{h=1}^{k-1} 2^{t-h} \times [g(h, k-1, n) \bmod 2]. \tag{18}$$

When producing an arbitrary superposed qudit state $|\phi\rangle = \sum_{k=0}^{2^t-1} a_k|k\rangle$, similar techniques can be employed, with the only difference being the positions where the coin operations are performed. Detailed discussions of these models are provided in Appendix C.

It is worth noting that even when combining a $(t-1)$-step QW using Model A with a single-step QW using Model B, we can still produce the target superposed state $|\phi\rangle = \sum_{k=0}^{2^t-1} a_k|k\rangle$. In essence, we treat the set $\{p_{t-1,0}, p_{t-1,1}, \ldots, p_{t-1,2^{t-1}-1}\}$ as the target probability distribution. After performing $t-1$ steps of a QW using Model A, this distribution is generated with spacing of 2 between adjacent positions. Then, by applying a single step of Model B, each position either remains unchanged or shifts one step to the right. As a result, we obtain a total of 2^t distinct positions with spacing 1, precisely corresponding to the target distribution.

Model C. (Time-dependent and position-dependent coins, varied shift length, three-state coin.)

Moreover, we can employ one-dimensional three-state QWs [70] to generate arbitrary probability distributions and superposed qudits. This approach reduces the total required steps from $t = \lceil \log_2 d \rceil$ to $t_1 = \lceil \log_3 d \rceil$. And the coin operations could further decrease.

The coin space is spanned by $\{|0\rangle, |1\rangle, |2\rangle\}$. The walker can either stand still, move backward, or move forward. The shift operation for general shift length is defined as follows:

$$S'_k = \sum_{n=-\infty}^{+\infty} (|n - l_k\rangle\langle n| \otimes |0\rangle\langle 0| + |n\rangle\langle n| \otimes |1\rangle\langle 1| + |n + l_k\rangle\langle n| \otimes |2\rangle\langle 2|). \tag{19}$$

The entire dynamics of the kth 1D three-state QW is given by

$$R_k = S'_k \cdot \left[\sum_{j=-\infty}^{+\infty} |j\rangle\langle j| \otimes C(k, j) \right]. \tag{20}$$

Here, $C(k, j)$ is a qutrit operation at position j. The details of the ternary structure and design of coin operations for probability distribution and qudit generation are discussed in Appendix D.

VI. NUMBER OF STEPS AND COIN OPERATIONS

Here, we count the number of steps in the QWs and the nonidentity coin operations required by each model.

To generate an arbitrary probability distribution $\{p_0, \ldots, p_{d-1}\}$, Model A (B) requires $t = \lceil \log_2 d \rceil$ QW steps and M_1 nonidentity coin operations, where

$$M_1 = 2^0 + \cdots + 2^{t-1} - (2^0 + \cdots + 2^{\lfloor \log(2^t - d) \rfloor - 1}) = 2^t - 2^{\lfloor \log(2^t - d) \rfloor}. \tag{21}$$

The subtraction accounts for the fact that coin operations can be arbitrary (or I) at nodes on the tree where the probability is zero. When the probability at a position $|j\rangle$ is zero, the corresponding amplitude is also zero. As a result, the evolved state contains a term $0|j\rangle \otimes (A_j|0\rangle + B_j|1\rangle)$, which remains zero regardless of the coin operator applied, even after the shift operator is applied.

Model C requires $t_1 = \lceil \log_3 d \rceil$ steps and M_2 nonidentity coin operations, where

$$M_2 = 3^0 + \cdots + 3^{t_1 - 1} - (3^0 + \cdots + 3^{\lfloor \log_3(3^{t_1} - d) \rfloor - 1}) = \tfrac{1}{2}(3^{t_1} - 3^{\lfloor \log_3(3^{t_1} - d) \rfloor}). \tag{22}$$

For generating an arbitrary qudit, using Model A(B), the total number of steps is $\lceil \log_2 d \rceil + 1$. With Technique 1, the number of nonidentity coin operations is $M_1 + d$, and with Technique 2, the number of nonidentity coin operations is $M_1 + \lceil d/2 \rceil \leqslant 5d/2$. For Model C, the total number of steps is $\lceil \log_3 d \rceil + 1$. With Technique 1, the number of coin operations is M_2, while with Technique 2, the number of coin operations is $M_2 + \lceil 2d/3 \rceil \leqslant 13d/6$. The number of coin operations for each model is plotted in Fig. 2.

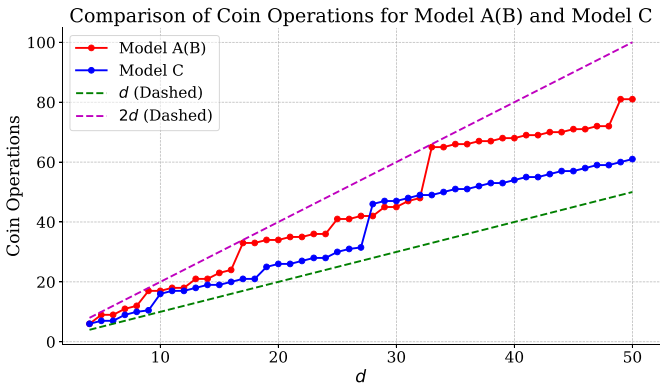


FIG. 2. Comparison of nonidentity coin operations required using Technique 2 for both binary tree and ternary tree structures, showing that both are $O(d)$. The red line represents Model A(B) using a binary tree structure, while the blue line represents Model C using a ternary tree structure.

VII. EXPERIMENT PROPOSAL

The proposals raised above are compatible with the developed integrated photonic quantum technologies. As an example, we demonstrate the implementation of Model B using an on-chip circuit. As Fig. 3 shows, the circuit consists of a mesh of variable beam splitters (VBS) and phase shifters. The thermo-optic phase shifter inserted in the path can introduce a phase shift of $[0, 2\pi)$. The VBS, realized using a Mach-Zehnder Interferometer (MZI) structure, is depicted in the inset of Fig. 3. By tuning the phase 2θ between the two arms of the MZI, an arbitrary binary probability distribution can be achieved for the output light when a beam is input from the input port. The VBS can be described with the unitary

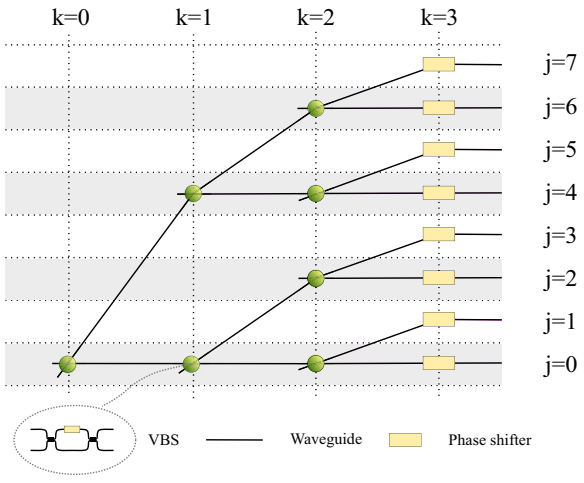


FIG. 3. Scheme for the proposed qudit preparation with integrated photonic platform. The green circle presents the variable beam splitter implemented with an MZI structure, as shown in the inset. For positions with zero amplitude, any coin operation would have no effect on the quantum state evolution and can therefore be set to the identity operator I, allowing these operations to be omitted, thus reducing resource consumption.

transformation as

$$C(k, j) = \begin{pmatrix} \cos\theta & -\sin\theta \\ \sin\theta & \cos\theta \end{pmatrix}.$$

In the proposed experimental setup, the VBS at each position is employed to implement the position-based coin operations of the 1D QW of Model B. The time-dependent shift operations are realized by directing the light into the desired positions with the corresponding silicon waveguides. In an actual on-chip circuit design, for each step, the optical path difference between the two waveguides orienting to two leaf nodes can be compensated by adjusting the length of the shorter one. At the final step, various phases are added to the corresponding paths to complete the preparation of the target qudit state.

VIII. COMPARISON WITH PREVIOUS WORKS

We now compare our new protocols with those developed in earlier research.

In [65], the shift length is fixed at 1. In contrast, our approach employs a variable shift length, reducing the total number of walk steps from $O(d)$ to $O(\log d)$ for arbitrary qudit preparation.

In [63], the dynamics of a 1D QW at step k are defined by $V_k = S \cdot (I \otimes C(k))$. This model employs only time-dependent coin operations, with a fixed shift length of 1. To generate a target qudit, the protocol requires designing $d-1$ coin operations $\{C(1), \ldots, C(d-1)\}$, an initial coin state $|\phi_c\rangle = a|0\rangle + b|1\rangle$, and a postselection coin state $|\phi_p\rangle = c|0\rangle + e|1\rangle$. The resulting unnormalized state $\langle\phi_p|V_{d-1}\cdots V_1|1\rangle \otimes |\phi_c\rangle$ approximates the target qudit up to normalization. Here, $|1\rangle$ is the initial walker state, the normalization factor relates to the success probability, and fidelity measures the closeness between the target and generated states.

Determining the $d-1$ coin operations involves solving $O(d)$ quadratic equations for the coefficients. It is claimed that almost all target qudits are reachable with high fidelity, excluding a measure-zero set. Solutions and coin states are generally nonunique. For $d > 5$, no general method exists to produce all solutions. The optimal average success probability is approximately 0.33 for $d \leqslant 5$. Numerical optimization has achieved success probabilities of $\geqslant$15% for $d \leqslant 20$ [63,64]. This approach requires $\frac{d(d-1)}{2}$ coin operations, with k identical nonidentity coin operations performed at different positions during the kth step.

In comparison, our protocols utilize a generalized 1D QW where the coin operators are both time- and position dependent, and the shift lengths vary with time. This allows fidelity and success probability to theoretically reach 1. Moreover, our protocols are computationally efficient and applicable to all qudits, as the dynamics are directly defined. Additionally, the number of required nonidentity coin operations decreases from $O(d^2)$ to $O(d)$.

Inspired by Ref. [63], two-dimensional quantum walk models have also been studied for generating quantum states [66]. For the preparation of qudit, only $O(\sqrt{d})$ steps two-dimensional quantum walk are required, thus reducing resources compared with Ref. [63]. However, our work further reduces the number of steps to $O(\log d)$ by introducing a varied shift lengths for one-dimensional quantum walks.

Compared to the circuit model for preparing arbitrary superposed qudits, certain physical systems allow for direct encoding into a d-level system, bypassing the need for entanglement between encoded n-qubit systems. Moreover, with the evolution steps reduced to $O(\log d)$, the preparation time is significantly shortened, as coin operations at different positions during each step of the QWs can be executed in parallel.

An interesting question is whether transforming the protocol for preparing superposition states in the QW model into the circuit model can also lead to a reduction in preparation time. In fact, when making this transformation, we cannot break the previous tight lower bound. The preparation of arbitrary n-qubit quantum states in the circuit model has been widely investigated. Without using ancillary qubits, the circuit depth (or preparation time) required is at least $O(2^n/n)$ [12].

To address the issue of exponential time consumption, a concept similar to that in computer science is adopted, namely trading space for time. To achieve a circuit depth of $O(n)$, $O(2^n)$ ancillary qubits are necessary [9,14]. Transforming the QW model into the circuit model is equivalent to adding an ancillary qubit as the coin space. The shift operation S_k in Eq. (16) (with $l_k = 1$) can be represented as $\mathcal{U}_{n,1} = \sum_{t=0}^{2^n-1}(I \otimes |0\rangle\langle 0| + |t+1 \bmod 2^n\rangle\langle t| \otimes |1\rangle\langle 1|)$. By generalizing the shift length to 2^l, the shift operation becomes

$$\mathcal{U}_{n,2^l} = \sum_{t=0}^{2^n-1}(I \otimes |0\rangle\langle 0| + |t+2^l \bmod 2^n\rangle\langle t| \otimes |1\rangle\langle 1|),$$

which, according to Eq. (D5) in Ref. [71], can be simplified to $\mathcal{U}_{n-l,1} \otimes I^{\otimes l}$. Although the transformed shift operator is easier to implement, there are still limitations in performing coin operations at different positions (represented as n bit strings). In the circuit model, coin operations at different positions cannot be carried out simultaneously.

IX. CONCLUSIONS

In this work, we have introduced efficient methods for the precise preparation of arbitrary probability distributions and superposed qudit states using 1D QWs with adjustable shift lengths. By constructing binary or ternary tree structures, we directly define the coin space operators in accordance with the desired probability distributions or qudit states. This approach achieves a total of $O(\log d)$ QW steps and requires $O(d)$ coin operations, offering a programmable and scalable solution for state preparation in quantum systems. Moreover, since coin operations at different positions can be executed in parallel, the overall preparation time is significantly reduced, further enhancing the efficiency of this $O(\log d)$-step QW evolution.

The ability to prepare arbitrary probability distributions is essential for a range of applications, including optimization algorithms, simulations in quantum computing, statistical physics, and machine learning. Furthermore, generating arbitrary quantum superposition states is fundamental for advancing quantum computing technologies, as it enables precise control and manipulation of quantum information.

While we mainly focus on preparing qudits in position space $\mathcal{H}_d$, it is possible to generate arbitrary entangled states in the position-coin space $\mathcal{H}_d \otimes \mathcal{H}_2$. For instance the superposed state is $\sum_{k=0}^{d-1} a_{k,0}|k\rangle|0\rangle + b_{k,1}|k\rangle|1\rangle$, where $\sum_{k=0}^{d-1}(|a_{k,0}|^2 + |b_{k,1}|^2) = 1$. The freedom to choose 2d complex parameters arbitrarily—subject to normalization—ensures that the entire space of pure entangled states in $\mathcal{H}_d \otimes \mathcal{H}_2$ can be covered. We can rewrite the state as $\sum_{k=0}^{d-1} a_k|k\rangle \otimes (\alpha_k|0\rangle + \beta_k|1\rangle)$, $|a_k|^2 = |a_{k,0}|^2 + |b_{k,1}|^2$, $\alpha_k = \frac{a_{k,0}}{a_k}$, $\beta_k = \frac{b_{k,1}}{a_k}$. If $a_k = 0$, we do not need to consider α_k and β_k as $a_{k,0} = b_{k,1} = 0$. A new QW step applied to the output state $\sum_{k=0}^{d-1} a_k|k\rangle \otimes |0\rangle$ is enough. We hope that the simple yet effective techniques presented here, based on 1D QWs, will prove useful for various quantum information processing tasks. Additionally, the variable-shift QW model proposed here may provide insights and offer new opportunities for further research in other areas of quantum information science.

ACKNOWLEDGMENTS

Y.W. acknowledges support from the National Natural Science Foundation of China (Grants No. 62001260 and No. 42330707) and the Beijing Natural Science Foundation (Grant No. Z220002). M.L. acknowledges support from the National Natural Science Foundation of China (Grant No. 62301531) and the Beijing Natural Science Foundation (Grant No. 4252012). Y.-Y.Z. acknowledges support from the Guangdong Provincial Quantum Science Strategic Initiative (Grants No. GDZX2403005 and No. GDZX2403002) and the Innovation Program for Quantum Science and Technology (Grant No. 2021ZD0302901).

APPENDIX A: PREVIOUSLY DISCUSSED 1D QW MODELS

We now provide a detailed introduction to the different models of 1D QW discussed in the literature.

Initially, one step of the simplest model of 1D QW is denoted as the following unitary operation [34,35]:

$$w_1 = T \cdot (I \otimes C). \tag{A1}$$

Here, T simulates the shift regulation,

$$T = \sum |n-1\rangle\langle n| \otimes |0\rangle\langle 0| + |n+1\rangle\langle n| \otimes |1\rangle\langle 1|. \tag{A2}$$

If the tossed coin is 0, the walker steps back from n to $n-1$. If it is 1, the walker steps ahead. The one-qubit unitary operation C regulates the probability of advancing or retreating. Usually, the Hadamard gate H is used as the unbiased operation controlling the movement of the walker.

Denote the initial state as $|\Psi\rangle = |0\rangle|0\rangle$.

Model 1: *A single coin.* In this model, the coin operations remain constant, independent of time and position. After N steps of the 1D QW, the output state is given by

$$w_1^N|\Psi\rangle.$$

Early studies utilizing this original model have explored various properties of the output state distributions, including probability distribution, hitting time, variance, and quantum speedup [72–74].

Model 2: *Time-dependent coins.* Here, the coin operations $C(k)$ are adjusted only based on the time step k. The dynamics of the kth step are described by

$$W_k = T \cdot (I \otimes C(k)).$$

After N steps of the QW, the evolved state is

$$|\Psi_N\rangle = W_N \cdots W_1|\Psi\rangle.$$

These coin types have been employed in [63,64] for qudit generation.

Model 3: *Position-dependent coins.* In this approach, the coin operations $C(j)$ are adjusted exclusively based on the position j. The dynamics of each step are governed by

$$W_1' = T \cdot \left(\sum_j |j\rangle\langle j| \otimes C(j)\right).$$

After N steps, the output state is

$$|\Psi_N\rangle = (W_1')^N|\Psi\rangle.$$

This model allows for tailored coin operations at specific positions, enabling more controlled QW dynamics.

Model 4: *Time- and position-dependent coins.* This comprehensive model adjusts the coin operations based on both time k and position j. The coin operation for the kth step at position j is defined as

$$I \otimes C(k) \to \sum_j |j\rangle\langle j| \otimes C(k, j).$$

The dynamics of the kth step are thus given by

$$W_k' = T \cdot \left(\sum_j |j\rangle\langle j| \otimes C(k, j)\right).$$

This model has been extensively utilized both theoretically and experimentally to simulate generalized positive operator-valued measures (POVMs) on qubits [67–69].

APPENDIX B: DETAILS OF PROBABILITY GENERATION AND QUDIT PREPARATION BY 1D QW WITH TWO DIRECTIONS

1. Probability generation

Here, we give a brief explanation to produce the arbitrary probability distribution by Model A. We can recursively observe the following property.

At the first step of the QW, we apply the coin operation $M(0, 0)$ at position 0, i.e., $C(1, 0) = M(0, 0)$. The shift length is 2^{t-1}. The evolved state is

$$|\Psi_1\rangle = W_1|\Psi\rangle = \sqrt{p_{1,0}}|-2^{t-1}\rangle \otimes |0\rangle + \sqrt{p_{1,1}}|2^{t-1}\rangle \otimes |1\rangle.$$

Here, the walker can be observed at either -2^{t-1} or 2^{t-1} with respective probabilities $p_{1,0}$ and $p_{1,1}$. Thus, the probability distribution $\{p_{1,0}, p_{1,1}\}$ is simulated at positions $\{-2^{t-1}, 2^{t-1}\}$, with an interval of 2^t between adjacent positions.

At the second step of the QW, we implement the coin operations $M(1, 0)$ at position -2^{t-1} for $p_{1,0}$ and $M(1, 1)X$ at position 2^{t-1} for $p_{1,1}$, denoted as $C(2, -2^{t-1}) = M(1, 0)$ and

$C(2, 2^{t-1}) = M(1,1)X$. The shift length is 2^{t-2}. The evolved state becomes

$$|\Psi_2\rangle = W_2|\Psi_1\rangle = \sqrt{p_{2,0}}|-3\times 2^{t-2}\rangle \otimes |0\rangle + \sqrt{p_{2,1}}|-2^{t-2}\rangle \otimes |1\rangle + \sqrt{p_{2,2}}|2^{t-2}\rangle \otimes |0\rangle + \sqrt{p_{2,3}}|3\times 2^{t-2}\rangle \otimes |1\rangle.$$

Measuring the position space of the evolved state yields the probabilities $\{p_{2,0}, p_{2,1}, p_{2,2}, p_{2,3}\}$ at positions $\{-3\times 2^{t-2}, -2^{t-2}, 2^{t-2}, 3\times 2^{t-2}\}$. The interval between each pair of adjacent positions is 2^{t-1}.

We will prove by mathematical induction that at the kth step, where $k = 1, 2, \ldots, t$, the evolved quantum state is given by

$$\begin{aligned}|\Psi_k\rangle &= W_k \cdots W_1|\Psi\rangle \\ &= \sum_{m=0}^{2^{k-1}-1} [\sqrt{p_{k,2m}}|2^{t-k} - 2^t + 4m\times 2^{t-k}\rangle \otimes |0\rangle \\ &\quad + \sqrt{p_{k,2m+1}}|2^{t-k} - 2^t + (4m+2)\times 2^{t-k}\rangle \otimes |1\rangle].\end{aligned} \tag{B1}$$

This means that, after k steps ($k = 1, 2, \ldots, t$) of the QW, measuring the position space will place the walker at 2^k distinct positions, ranging from the leftmost position $-(2^{t-1} + 2^{t-2} + \cdots + 2^{t-k}) = 2^{t-k}(1-2^k)$ to the rightmost position $2^{t-1} + 2^{t-2} + \cdots + 2^{t-k} = 2^{t-k}(2^k - 1)$. The interval between two adjacent positions is 2^{t-k+1}, with corresponding probabilities $\{p_{k,0}, p_{k,1}, \ldots, p_{k,2^k-1}\}$. Each superposition position corresponds to a possible destination after $k-1$ steps of the QW.

For the base case [$k = 1$ in Eq. (B1)], the state $|\Psi_1\rangle$ follows the form.

As at the $(k+1)$th step, the shift length is designed as $2^{t-(k+1)}$ and the coin operations are $M(k,n)X^n$ from the leftmost position for $p_{k,0}$ to the rightmost position for $p_{k,2^k-1}$. The coin operations part is equal to perform coin operation $M(k, 2m)$ at position $2^{t-k} - 2^t + 4m\times 2^{t-k}$, and perform $M(k, 2m+1)X$ at position $2^{t-k} - 2^t + (4m+2)\times 2^{t-k}$.

After these coin operations on $|\Psi_k\rangle$, denoted as $U_{c,k}$, the evolved state is given by

$$\begin{aligned}U_{c,k}|\Psi_k\rangle = \sum_{m=0}^{2^{k-1}-1} &[|2^{t-k} - 2^t + 4m\times 2^{t-k}\rangle \otimes (\sqrt{p_{k+1,4m}}|0\rangle \\ &+ \sqrt{p_{k+1,4m+1}}|1\rangle) + |2^{t-k} - 2^t \\ &+ (4m+2)\times 2^{t-k}\rangle \otimes (\sqrt{p_{k+1,4m+2}}|0\rangle \\ &+ \sqrt{p_{k+1,4m+3}}|1\rangle)].\end{aligned} \tag{B2}$$

Then after the shift operation T_{k+1}, where the shift length $l_{k+1} = 2^{t-(k+1)}$, the state will be

$$\begin{aligned}|\Psi_{k+1}\rangle &= W_{k+1}|\Psi_k\rangle = T_{k+1}U_{c,k}|\Psi_k\rangle \\ &= \sum_{m=0}^{2^{k-1}-1} [\sqrt{p_{k+1,4m}}|2^{t-k} - 2^t + (8m-1)\times 2^{t-k-1}\rangle \otimes |0\rangle + \sqrt{p_{k+1,4m+1}}|2^{t-k} - 2^t + (8m+1)\times 2^{t-k-1}\rangle \otimes |1\rangle] \\ &\quad + \sqrt{p_{k+1,4m+2}}|2^{t-k} - 2^t + (8m+4-1)\times 2^{t-k-1}\rangle \otimes |0\rangle] + \sqrt{p_{k+1,4m+3}}|2^{t-k} - 2^t + (8m+4+1)\times 2^{t-k-1}\rangle \otimes |1\rangle] \\ &= \sum_{m=0}^{2^{k-1}-1} [\sqrt{p_{k+1,4m}}|2^{t-k-1} - 2^t + 8m\times 2^{t-k-1}\rangle \otimes |0\rangle + \sqrt{p_{k+1,4m+1}}|2^{t-k-1} - 2^t + (8m+2)\times 2^{t-k-1}\rangle \otimes |1\rangle] \\ &\quad + \sqrt{p_{k+1,4m+2}}|2^{t-k-1} - 2^t + (8m+4)\times 2^{t-k-1}\rangle \otimes |0\rangle] + \sqrt{p_{k+1,4m+3}}|2^{t-k-1} - 2^t + (8m+6)\times 2^{t-k-1}\rangle \otimes |1\rangle] \\ &= \sum_{m=0}^{2^k-1} [\sqrt{p_{k+1,2m}}|2^{t-k-1} - 2^t + 4m\times 2^{t-k-1}\rangle \otimes |0\rangle + \sqrt{p_{k+1,2m+1}}|2^{t-k-1} - 2^t + (4m+2)\times 2^{t-k-1}\rangle \otimes |1\rangle].\end{aligned}$$

Therefore, by induction, the evolution of the quantum state at each step follows the expected form in Eq. (B1) for all steps k. This completes the proof.

It is easy to observe that, during the probability distribution generation process $\{p_{k,0}, p_{k,1}, \ldots, p_{k,2^k-1}\}$, the coin state corresponding to $p_{k,2m}$ is $|0\rangle$, while the coin state corresponding to $p_{k,2m+1}$ is $|1\rangle$.

After t steps ($k = t$ in Eq. (B1)), the final state is

$$\begin{aligned}|\Psi_t\rangle &= W_t \cdots W_1|\Psi\rangle \\ &= \sum_{m=0}^{2^{t-1}-1} [\sqrt{p_{t,2m}}|-2^t + 1 + 4m\rangle \otimes |0\rangle + \sqrt{p_{t,2m+1}}|-2^t + 3 + 4m\rangle \otimes |1\rangle] \\ &= \sum_{m=0}^{2^{t-1}-1} [\sqrt{p_{2m}}|-2^t + 1 + 4m\rangle \otimes |0\rangle + \sqrt{p_{2m+1}}|-2^t + 3 + 4m\rangle \otimes |1\rangle].\end{aligned} \tag{B3}$$

Projecting the position space onto the basis states $\{\ldots, |-1\rangle, |0\rangle, |1\rangle, \ldots\}$ results in the walker being found at position $-2^t + 1 + 2k$ with probability p_k. This means that the target probability distribution $\{p_0, p_1, \ldots, p_{2^t-1}\}$ is achieved at positions $\{-2^t + 1, -2^t + 3, \ldots, 2^t - 3, 2^t - 1\}$.

2. Example

Let us consider a probability distribution $\{p_0 = \frac{1}{4}, p_1 = \frac{1}{4}, p_2 = \frac{1}{4}, p_3 = \frac{1}{4}\}$.

First, we construct the corresponding binary tree based on the probability distribution. The leaf nodes at the bottom level of the tree take the values $\{p_{2,0} = p_{2,1} = p_{2,2} = p_{2,3} = \frac{1}{4}\}$. Moving up one level, the parent nodes are given by $\{p_{1,0} = p_{2,1} = \frac{1}{2}\}$. Finally, at the root node, we have $p_{0,0} = 1$.

Since there are four probability values, we need to perform $t = \log 4 = 2$ steps of quantum walk. The step length for the shift operator is directly defined according to the total walk steps t: it is 2 for the first step and 1 for the second step.

The coin operator is defined by the values of the binary tree.

At $k = 1$, the system's initial state is $|0\rangle|0\rangle$. We apply a Hadamard operator on position $|0\rangle$, and after applying the shift operator with a step length of 2, the evolved state becomes

$$\frac{1}{\sqrt{2}}(|-2\rangle|0\rangle + |2\rangle|1\rangle).$$

At $k = 2$, we apply a Hadamard operator H at position $|-2\rangle$ and a HX coin operator at position $|2\rangle$. After applying the shift operator with a step length of 1, the final state becomes

$$\tfrac{1}{2}(|-3\rangle|0\rangle + |-1\rangle|1\rangle + |1\rangle|0\rangle + |3\rangle|1\rangle).$$

When we perform a projective measurement in position space, the probabilities for the walker to be at positions -3, -1, 1, and 3 are all $\frac{1}{4}$.

To generate any arbitrary probability distribution, we can adjust the values at the binary tree nodes accordingly. Then, based on the corresponding node unitary operations, we design different coin operators for various positions and walk times.

3. Qudit generation

The final state that achieves the desired probability distribution after t steps is presented in Eq. (B3). The following two techniques can be employed to transform this probability distribution protocol into a qudit preparation protocol, as discussed above.

Technique 1. First, obtain the state in Eq. (B3) using the probability generation method. Then, add a $(t+1)$th step to the 1D QWs. Apply the following coin operations:

(1) $C(t+1, -2^t + 1 + 4m) = e^{i\theta_{2m}}|0\rangle\langle 0| + |1\rangle\langle 1|$,

(2) $C(t+1, -2^t + 3 + 4m) = e^{i\theta_{2m+1}}|0\rangle\langle 1| + |1\rangle\langle 0|$,

where $m = 0, \ldots, 2^{t-1} - 1$. The shift length for the $(t+1)$th step is set to 0. Consequently, the updated final state is

$$\begin{aligned}|\Psi'_{t+1}\rangle &= W'_{t+1}W_t \cdots W_1|\Psi\rangle \\ &= \sum_{m=0}^{2^t-1} \sqrt{p_m}e^{i\theta_m}|-2^t + 1 + 2m\rangle \otimes |0\rangle. \end{aligned} \tag{B4}$$

As we have expressed the complex number $a_m = \sqrt{p_m}e^{i\theta_m}$, the final state is exactly $|\phi\rangle \otimes |0\rangle$, ensuring that the target state $|\phi\rangle$ is prepared in the position space with a probability of 1.

Technique 2. Alternatively, we can optimize the protocol by modifying the coin operations at both the tth and $(t+1)$th steps. After $t-1$ steps of the 1D QW, the final state is

$$\begin{aligned}|\Psi_{t-1}\rangle = \sum_{m=0}^{2^{t-2}-1} &[\sqrt{p_{t-1,2m}}|-2^t + 2 + 8m\rangle \otimes |0\rangle \\ &+ \sqrt{p_{t-1,2m+1}}|-2^t + 6 + 8m\rangle \otimes |1\rangle]. \end{aligned} \tag{B5}$$

At the tth step, sequentially from the leftmost to the rightmost position, we modify the coin operations in Eq. (9) at each position to

$$Z_n M(t-1, n) X^n, \tag{B6}$$

where

$$Z_n = e^{i\theta_{2n}}|0\rangle\langle 0| + e^{i\theta_{2n+1}}|1\rangle\langle 1|. \tag{B7}$$

The shift length at step t remains $l_t = 1$. The evolved state then becomes

$$\begin{aligned}|\Psi'_t\rangle &= W'_t W_{t-1} \cdots W_1|\Psi\rangle \\ &= \sum_{m=0}^{2^{t-1}-1} [\sqrt{p_{2m}}e^{i\theta_{2m}}|-2^t + 1 + 4m\rangle \otimes |0\rangle \\ &\quad + \sqrt{p_{2m+1}}e^{i\theta_{2m+1}}|-2^t + 3 + 4m\rangle \otimes |1\rangle]. \end{aligned} \tag{B8}$$

These phase differences are now fixed as shown in Eq. (B8).

To finalize the state, at the $(t+1)$th step of the QW, we perform the coin operation X at each position $-2^t + 3 + 4m$, where $m = 0, \ldots, 2^{t-1} - 1$. The shift length for the $(t+1)$th step is set to 0, resulting in the final state as described in Eq. (B4).

4. Example

Suppose we want to generate the qudit state

$$|\phi\rangle = \tfrac{1}{2}(|-3\rangle + i|-1\rangle - |1\rangle + e^{2\pi i/3}|3\rangle).$$

First, we need to generate the state for the probability distribution $\{p_0 = p_1 = p_2 = p_3 = 1/4\}$, as described in Appendix B 2.

Technique 1. We introduce a new quantum walk (QW) step on the output state,

$$\tfrac{1}{2}(|-3\rangle|0\rangle + |-1\rangle|1\rangle + |1\rangle|0\rangle + |3\rangle|1\rangle).$$

At the positions $|-3\rangle, |-1\rangle, |1\rangle, |3\rangle$, we apply coin operators to change the coin states $|0\rangle, |1\rangle, |0\rangle, |1\rangle$ into $|0\rangle, i|0\rangle, -|0\rangle, e^{2\pi i/3}|0\rangle$, respectively. Then, we set the shift length to 0. This results in the final state,

$$|\phi\rangle \otimes |0\rangle.$$

Technique 2: We modify the coin operators by Eq. (B6) at step $k = 2$ for the output state,

$$\frac{1}{\sqrt{2}}(|-2\rangle|0\rangle + |2\rangle|1\rangle).$$

Specifically:

(1) The coin operator at position $|-2\rangle$ is changed from H to

$$\frac{1}{\sqrt{2}}[(|0\rangle + i|1\rangle)\langle 0| + (|0\rangle - i|1\rangle)\langle 1|].$$

(2) The coin operator at position $|2\rangle$ is changed from H to

$$\frac{1}{\sqrt{2}}[(-|0\rangle + e^{2\pi i/3}|1\rangle)\langle 0| - (|0\rangle + e^{2\pi i/3}|1\rangle)\langle 1|]X.$$

The shift length is set to 1. After this updated QW step, the state evolves to

$$\tfrac{1}{2}(|-3\rangle|0\rangle + i|-1\rangle|1\rangle - |1\rangle|0\rangle + e^{2\pi i/3}|3\rangle|1\rangle).$$

At step $k = 3$, we only need to set the coin operators at positions $|-1\rangle$ and $|3\rangle$ to X. The shift length is set to 0. By doing so, half of the coin operators at $k = 3$ are saved, and the target state $|\phi\rangle \otimes |0\rangle$ can be successfully obtained.

APPENDIX C: DETAILS OF PROBABILITY GENERATION AND QUDIT PREPARATION BY 1D QW WITH A SINGLE DIRECTION

1. Probability generation

The designs for 1D QW (Model B) mirror our earlier discussion on 1D QW in two directions (Model A). The total number of steps remains $t = \lceil \log_2 d \rceil$. At each step $k = 1, \cdots, t$, the shift length remains 2^{t-k}. The coin operations are related to the node operations $M(m, n)$, following the binary tree structure. The only difference lies in the positions where we apply the coin operations.

At the first step of QWs, the coin operation at position 0 is $C(1, 0) = M(0, 0)$. The evolved state will be

$$|\Psi_1\rangle = V_1|\Psi\rangle = \sqrt{p_{1,0}}|0\rangle \otimes |0\rangle + \sqrt{p_{1,1}}|2^{t-1}\rangle \otimes |1\rangle.$$

The walker can be found at position 0 with probability $p_{1,0}$, or at position 2^{t-1} with probability $p_{1,1}$. The interval of the positions is 2^{t-1}.

At the second step of QWs, the coin operation at position 0 is given by $C(2, 0) = M(1, 0)$, and the coin operation at position 2^{t-1} is $C(2, 2^{t-1}) = M(1, 1)X$. The evolved quantum state is then expressed as

$$\begin{aligned}|\Psi_2\rangle = V_2|\Psi_1\rangle = &\sqrt{p_{2,0}}|0\rangle \otimes |0\rangle + \sqrt{p_{2,1}}|2^{t-2}\rangle \otimes |1\rangle \\ &+ \sqrt{p_{2,2}}|2^{t-1}\rangle \otimes |0\rangle \\ &+ \sqrt{p_{2,3}}|2^{t-1} + 2^{t-2}\rangle \otimes |1\rangle.\end{aligned}$$

Thus, the walker can be found at positions 0, 2^{t-2}, $2 \times 2^{t-2}$, or $3 \times 2^{t-2}$. The interval between these positions is 2^{t-2}.

In general, at the kth step of QWs, where $k = 1, \ldots, t$, we perform coin operations $M(k-1, n)X^n$ from the leftmost position to the rightmost position, where $n = 0, 1, \ldots, 2^k - 1$. With the shift regulation by Eq. (16), the leftmost position at each step remains fixed at 0. Similar to the earlier discussion, we can obtain the probability distribution $\{p_{k,0}, p_{k,1}, \cdots, p_{k,2^k-1}\}$ from the leftmost position 0 to the rightmost position $2^{t-k}(2^k - 1)$. The interval of two adjacent positions becomes 2^{t-k}.

After t steps of QWs, the rightmost position is $2^t - 1$. We will obtain the state

$$\begin{aligned}|\Psi_t\rangle &= V_t \cdots V_1|\Psi\rangle \\ &= \sum_{m=0}^{2^{t-1}-1} [\sqrt{p_{t,2m}}|2m\rangle \otimes |0\rangle + \sqrt{p_{t,2m+1}}|2m+1\rangle \otimes |1\rangle] \\ &= \sum_{m=0}^{2^{t-1}-1} [\sqrt{p_{2m}}|2m\rangle \otimes |0\rangle + \sqrt{p_{2m+1}}|2m+1\rangle \otimes |1\rangle].\end{aligned} \tag{C1}$$

We then take projective measurement at position space onto the states $\{\cdots, |-1\rangle, |0\rangle, |1\rangle, \cdots\}$. The walker will be found at position j with probability p_j.

2. Qudit preparation

With the single direction model, we can use two similar methods to produce an arbitrary qudit state $|\phi\rangle = \sum_{k=0}^{d-1} a_k|k\rangle = \sum_{k=0}^{d-1} \sqrt{p_k}e^{i\theta_k}|k\rangle$, where $p_k = |a_k|^2$ and $\theta_k \in [0, 2\pi)$.

Technique 1. First, we use a total of t steps of a 1D QW to obtain the state in Eq. (C1). Then, at the $(t+1)$th step, we perform the following new coin operations,

(1) $C(t+1, 2m) = e^{i\theta_{2m}}|0\rangle\langle 0| + |1\rangle\langle 1|$,

(2) $C(t+1, 2m+1) = e^{i\theta_{2m+1}}|0\rangle\langle 1| + |1\rangle\langle 0|$,

where $m = 0, \cdots, 2^t - 1$. This results in the state

$$|\Psi'_{t+1}\rangle = V'_{t+1}V_t \cdots V_1|\Psi\rangle = \sum_{k=0}^{2^t-1} \sqrt{p_k}e^{i\theta_k}|k\rangle \otimes |0\rangle. \tag{C2}$$

The state at the position space is the target state to be generated.

Technique 2. We modify the coin operations at the tth and $(t+1)$th step. At the end of the $(t-1)$th step of the 1D QW to generate the probability distribution, the evolved state is given by

$$\begin{aligned}|\Psi_{t-1}\rangle &= V_{t-1} \cdots V_1|\Psi\rangle \\ &= \sum_{n=0}^{2^{t-2}-1} [\sqrt{p_{t-1,2n}}|4n\rangle \otimes |0\rangle \\ &\quad + \sqrt{p_{t-1,2n+1}}|4n+2\rangle \otimes |1\rangle].\end{aligned} \tag{C3}$$

At the tth step of QWs, we set the coin operations as $\{Z_n M(t-1, n)X^n : n = 0, \cdots, 2^{t-1} - 1\}$ from the leftmost position 0 to the rightmost position $2^t - 1$ with interval 2. Here Z_n is defined in Eq. (B7). After the tth step, we obtain the state

$$\begin{aligned}|\Psi'_t\rangle &= V'_t V_{t-1} \cdots V_1|\Psi\rangle \\ &= \sum_{m=0}^{2^{t-1}-1} [\sqrt{p_{2m}}e^{i\theta_{2m}}|2m\rangle \otimes |0\rangle \\ &\quad + \sqrt{p_{2m+1}}e^{i\theta_{2m+1}}|2m+1\rangle \otimes |1\rangle].\end{aligned} \tag{C4}$$

Similarly, at the $(t+1)$th step, we set the coin operation as X for position $2m+1$, where $m = 0, \cdots, 2^{t-1} - 1$. Then we will obtain the same state in Eq. (C2).

APPENDIX D: ONE-DIMENSIONAL THREE STATES QWS AND TERNARY TREE STRUCTURE

1. Probability generation

Here, we give a brief explanation to produce the arbitrary probability distribution by Model C.

We define a ternary tree similar to the one in Fig. 1. For an arbitrary probability distribution $\{p_1, \cdots, p_{d-1}\}$, we put it to the leaf nodes as $\{p_{t_1,0}, \cdots, p_{t_1,3^{t_1}-1}\}$ in sequence. Each parent node in the tree has three child nodes, and the sum of the values of the child nodes equals the value of the parent node.

Each node can define a 3×3 unitary node operation.

$$M_1(m, n) = \frac{1}{\sqrt{p_{m,n}}} \begin{pmatrix} \sqrt{p_{m+1,3n}} & * & * \\ \sqrt{p_{m+1,3n+1}} & * & * \\ \sqrt{p_{m+1,3n+2}} & * & * \end{pmatrix}. \tag{D1}$$

Through the Gram-Schmidt orthogonalization process, we have flexibility in choosing the value of $*$ to ensure that $M_1(m,n)$ becomes unitary.

Shift length. At the kth step of 1D QW, $k = 1, \cdots, t_1$, we set the shift length as $l_k = 3^{t_1-k}$.

Coin operations. At the kth step of 1D QW, the coin operations are $\{M_1(k-1,n)X_1^n, n = 0, \cdots, 3^{k-1}-1\}$ from the leftmost position to the rightmost position of the walker. Here the operation X_1 is the following:

$$X_1 = |0\rangle\langle 1| + |1\rangle\langle 2| + |2\rangle\langle 0|. \tag{D2}$$

The position for coin operations at step k. To determine the position j for coin operation $\{M_1(k-1,n)X_1^n, n = 0, \cdots, 3^{k-1}-1\}$, we should find a path from the root node $p_{0,0}$ to the leaf node $p_{k-1,n}$ on the ternary tree,

$$j = \sum_{h=1}^{k-1} 3^{t_1-h} \times [(g(h,k-1,n) \bmod 3) - 1]. \tag{D3}$$

Similarly, after k steps, we obtain the probability distribution $\{p_{k,0}, p_{k,1}, \ldots, p_{k,3^k-1}\}$. In the final step t_1, the target probability distribution is simulated. Also, two techniques can be employed to transform the probability generation protocol into a qudit generation protocol.

At the first step of QWs, we use the coin operation $M_1(0,0)$ at position 0. Namely, $C(1,0) = M_1(0,0)$. The evolved state will be

$$|\Psi_1\rangle = R_1|\Psi\rangle = \sqrt{p_{1,0}}|-3^{t_1-1}\rangle \otimes |0\rangle + \sqrt{p_{1,1}}|0\rangle \otimes |1\rangle + \sqrt{p_{1,2}}|3^{t_1-1}\rangle \otimes |0\rangle.$$

The walker's position can be observed at either -3^{t_1-1}, 0 or 3^{t_1-1} with probabilities $p_{1,0}$, $p_{1,1}$ or $p_{1,2}$ correspondingly. Thus the probability distribution $\{p_{1,0}, p_{1,1}, p_{1,2}\}$ is generated at position $\{-3^{t_1-1}, 0, 3^{t_1-1}\}$. The interval of two adjacent positions is 3^{t_1-1}.

At the second step of the QWs, we implement the coin operations $M_1(1,0)$ at position -3^{t_1-1}, $M_1(1,1)X_1$ at position 0, and $M_1(1,2)X_1^2$ at position 3^{t_1-1}. They are denoted as $C(2,-3^{t_1-1}) = M_1(1,0)$, $C(2,0) = M_1(1,1)X_1$ and $C(2,3^{t_1-1}) = M_1(1,2)X_1^2$. The evolved state is given by

$$\begin{aligned}|\Psi_2\rangle = R_2|\Psi_1\rangle = {} & \sqrt{p_{2,0}}|-4h\rangle \otimes |0\rangle + \sqrt{p_{2,1}}|-3h\rangle \otimes |1\rangle \\ & + \sqrt{p_{2,2}}|-2h\rangle \otimes |2\rangle + \sqrt{p_{2,3}}|-h\rangle \otimes |0\rangle \\ & + \sqrt{p_{2,4}}|0\rangle \otimes |1\rangle + \sqrt{p_{2,5}}|h\rangle \otimes |2\rangle \\ & + \sqrt{p_{2,6}}|2h\rangle \otimes |0\rangle + \sqrt{p_{2,7}}|3h\rangle \otimes |1\rangle \\ & + \sqrt{p_{2,8}}|4h\rangle \otimes |2\rangle.\end{aligned}$$

Here, $h = 3^{t_1-2}$. If we measure the position space of the evolved state, we can obtain the probabilities $\{p_{2,0}, \cdots, p_{2,8}\}$ at position $\{-4h, -3h, \cdots, 3h, 4h\}$. The interval of each two adjacent positions is $h = 3^{t_1-2}$.

At the end of kth step ($k = 1, 2 \cdots, t$) of QWs, if we measure the position space, the walker could be found at the 3^k different positions from the leftmost position $-(3^{t_1-1} + 3^{t_1-2} + \cdots + 3^{t_1-k}) = 3^{t_1-k} \times (\frac{1-3^k}{2})$ to the rightmost position $3^{t_1-1} + 3^{t_1-2} + \cdots + 2^{t_1-k} = 3^{t_1-k} \times (\frac{3^k-1}{2})$. The interval of two adjacent positions is 3^{t_1-k}. The corresponding probabilities are $\{p_{k,0}, p_{k,1}, \cdots, p_{k,3^k-1}\}$.

During the process of generating the probability distribution $\{p_{k,0}, p_{k,1}, \ldots, p_{k,3^k-1}\}$, the coin state for the position corresponding to $p_{k,3m}$ is $|0\rangle$. The coin state for the position corresponding to $p_{k,3m+1}$ is $|1\rangle$, and the coin state for the position corresponding to $p_{k,3m+2}$ is $|2\rangle$.

After t steps, the final state arrives at

$$\begin{aligned}|\Psi_t\rangle &= R_t \cdots R_1|\Psi\rangle \\ &= \sum_{m=0}^{3^{t_1-1}-1} \left[\sqrt{p_{t,3m}}|\frac{1-3^{t_1}}{2} + 3m\rangle \otimes |0\rangle + \sqrt{p_{t,3m+1}}|\frac{1-3^{t_1}}{2} + 3m+1\rangle \otimes |1\rangle + \sqrt{p_{t,3m+2}}|\frac{1-3^{t_1}}{2} + 3m+2\rangle \otimes |2\rangle\right] \\ &= \sum_{m=0}^{3^{t_1-1}-1} \left[\sqrt{p_{3m}}|\frac{1-3^{t_1}}{2} + 3m\rangle \otimes |0\rangle + \sqrt{p_{3m+1}}|\frac{1-3^{t_1}}{2} + 3m+1\rangle \otimes |1\rangle + \sqrt{p_{3m+2}}|\frac{1-3^{t_1}}{2} + 3m+2\rangle \otimes |2\rangle\right].\end{aligned} \tag{D4}$$

If we project the position space with states $\{\cdots, |-1\rangle, |0\rangle, |1\rangle, \cdots\}$, the walker will be in position $\frac{1-3^{t_1}}{2} + k$ with probability p_k. It means that we can obtain the target probability distribution $\{p_0, \cdots, p_{3^{t_1}-1}\}$ at positions $\{\frac{1-3^{t_1}}{2}, \frac{3-3^{t_1}}{2}, \cdots, \frac{3^{t_1}-3}{2}, \frac{3^{t_1}-1}{2}\}$.

When the initial state is changed to $|\Psi'\rangle = |\frac{3^{t_1}-1}{2}\rangle \otimes |0\rangle$, we can obtain the walker at position k with probability p_k. The evolved state will be

$$|\Psi_t\rangle = R_t \cdots R_1|\Psi'\rangle = \sum_{m=0}^{3^{t_1-1}-1} [\sqrt{p_{3m}}|3m\rangle \otimes |0\rangle + \sqrt{p_{3m+1}}|3m+1\rangle \otimes |1\rangle + \sqrt{p_{3m+2}}|3m+2\rangle \otimes |2\rangle]. \tag{D5}$$

2. Qudit generation

Now we use the Model C to produce an arbitrary qudit state $|\phi\rangle = \sum_{k=0}^{d-1} a_k|k\rangle = \sum_{k=0}^{d-1} \sqrt{p_k}e^{i\theta_k}|k\rangle$, where $p_k = |a_k|^2$ and $\theta_k \in [0, 2\pi)$. This state is encoded as $|\phi\rangle = \sum_{k=0}^{3^{t_1}-1} \sqrt{p_k}e^{i\theta_k}|k\rangle$.

Technique 1. First, we use a total of t steps of a 1D QW to obtain the state in Eq. (D5). Then, at the (t_1+1)th step, we perform the following new coin operations:

(1) $C(t+1,3m) = e^{i\theta_{3m}}|0\rangle\langle 0| + |1\rangle\langle 1| + |2\rangle\langle 2|$,
(2) $C(t+1,3m+1) = e^{i\theta_{3m+1}}|0\rangle\langle 1| + |1\rangle\langle 0| + |2\rangle\langle 2|$,
(3) $C(t+1,3m+2) = e^{i\theta_{3m+2}}|0\rangle\langle 2| + |2\rangle\langle 0| + |1\rangle\langle 1|$,

where $m = 0, \cdots, 3^{t_1} - 1$. This results in the state,

$$|\Psi'_{t_1+1}\rangle = R'_{t_1+1}R_{t_1}\cdots R_1|\Psi'\rangle = \sum_{k=0}^{3^{t_1}-1}\sqrt{p_k}e^{i\theta_k}|k\rangle\otimes|0\rangle. \tag{D6}$$

The state at the position space is the target state to be generated.

Technique 2. We modify the coin operations at the t_1th and (t_1+1)th step. At the end of the (t_1-1)th step of the 1D QW to generate the probability distribution, the evolved state is given by

$$\left|\Psi_{t_1-1}\right\rangle = R_{t-1}\cdots R_1|\Psi'\rangle = \sum_{m=0}^{3^{t_1-2}-1}\left[\sqrt{p_{t_1-1,3m}}|1+9m\rangle\otimes|0\rangle + \sqrt{p_{t_1-1,3m+1}}|4+9m\rangle\otimes|1\rangle + \sqrt{p_{t_1-1,3m+2}}|7+9m\rangle\otimes|2\rangle\right]. \tag{D7}$$

At the t_1th step of QWs, we sequentially set the coin operations as $\{Z'_nM_1(t_1-1,n)X_1^n : n = 0, \cdots, 3^{t_1-1}-1\}$ from the leftmost position 1 to the rightmost position with interval 3. Here Z'_n is defined as follows:

$$Z'_n = e^{i\theta_{3n}}|0\rangle\langle 0| + e^{i\theta_{3n+1}}|1\rangle\langle 1| + e^{i\theta_{3n+2}}|2\rangle\langle 2|. \tag{D8}$$

After the t_1th step, we obtain the state

$$\left|\Psi'_{t_1}\right\rangle = R'_{t_1}R_{t_1-1}\cdots R_1|\Psi'\rangle = \sum_{m=0}^{3^{t_1-1}-1}[\sqrt{p_{3m}}e^{i\theta_{3m}}|3m\rangle\otimes|0\rangle + \sqrt{p_{3m+1}}e^{i\theta_{3m+1}}|3m+1\rangle\otimes|1\rangle + \sqrt{p_{3m+2}}e^{i\theta_{3m+2}}|3m+2\rangle\otimes|2\rangle]. \tag{D9}$$

Similarly, at the (t_1+1)th step, we set the coin operation as X_1 for position $3m+1$ and X_1^2 for position $3m+2$. Then we will obtain the same state in Eq. (D6).

[1] D. J. Wineland, Nobel lecture: Superposition, entanglement, and raising Schrödinger's cat, Rev. Mod. Phys. **85**, 1103 (2013).

[2] K. Modi, A. Brodutch, H. Cable, T. Paterek, and V. Vedral, The classical-quantum boundary for correlations: Discord and related measures, Rev. Mod. Phys. **84**, 1655 (2012).

[3] D. Cozzolino, B. Da Lio, D. Bacco, and L. K. Oxenløwe, High-dimensional quantum communication: Benefits, progress, and future challenges, Adv. Quantum Technol. **2**, 1900038 (2019).

[4] M. X. Luo and X. J. Wang, Universal quantum computation with qudits, Sci. China Phys. Mech. Astron. **57**, 1712 (2014).

[5] J. Biamonte, P. Wittek, N. Pancotti, P. Rebentrost, N. Wiebe, and S. Lloyd, Quantum machine learning, Nature (London) **549**, 195 (2017).

[6] A. S. Nikolaeva, E. O. Kiktenko, and A. K. Fedorov, Efficient realization of quantum algorithms with qudits, EPJ Quantum Tech. **11**, 43 (2024).

[7] M. A. Nielsen and I. L. Chuang, *Quantum Computation and Quantum Information* (Cambridge University Press, Cambridge, 2010).

[8] M. Plesch and Č. Brukner, Quantum-state preparation with universal gate decompositions, Phys. Rev. A **83**, 032302 (2011).

[9] X.-M. Zhang, T. Li, and X. Yuan, Quantum state preparation with optimal circuit depth: Implementations and applications, Phys. Rev. Lett. **129**, 230504 (2022).

[10] G.-L. Long and Y. Sun, Efficient scheme for initializing a quantum register with an arbitrary superposed state, Phys. Rev. A **64**, 014303 (2001).

[11] V. V. Shende, S. S. Bullock, and I. L. Markov, Synthesis of quantum logic circuits, IEEE Trans. Comput.-Aided Des. Integr. Circuits Syst. **25**, 1000 (2006).

[12] X. Sun, G. Tian, S. Yang, P. Yuan, and S. Zhang, Asymptotically optimal circuit depth for quantum state preparation and general unitary synthesis, IEEE Trans. Comput.-Aided Des. Integr. Circuits Sys. **42**, 3301 (2023).

[13] A. Bärtschi and S. Eidenbenz, Short-depth circuits for dicke state preparation, in *2022 IEEE International Conference on Quantum Computing and Engineering (QCE)* (IEEE, 2022), pp. 87–96.

[14] P. Yuan and S. Zhang, Optimal (controlled) quantum state preparation and improved unitary synthesis by quantum circuits with any number of ancillary qubits, Quantum **7**, 956 (2023).

[15] D. A. Puente, F. Motzoi, T. Calarco, G. Morigi, and M. Rizzi, Quantum state preparation via engineered ancilla resetting, Quantum **8**, 1299 (2024).

[16] N. Gleinig and T. Hoefler, An efficient algorithm for sparse quantum state preparation, in *2021 58th ACM/IEEE Design Automation Conference (DAC)* (IEEE, 2021), pp. 433–438.

[17] L. Li and J. Luo, Nearly optimal circuit size for sparse quantum state preparation, arXiv:2406.16142.

[18] M. Cerezo, A. Arrasmith, R. Babbush, S. C. Benjamin, S. Endo, K. Fujii, J. R. McClean, K. Mitarai, X. Yuan, L. Cincio *et al.*, Variational quantum algorithms, Nat. Rev. Phys. **3**, 625 (2021).

[19] B. T. Gard, L. Zhu, G. S. Barron, N. J. Mayhall, S. E. Economou, and E. Barnes, Efficient symmetry-preserving state preparation circuits for the variational quantum eigensolver algorithm, npj Quantum Inf. **6**, 10 (2020).

[20] A. Holmes and A. Y. Matsuura, Efficient quantum circuits for accurate state preparation of smooth, differentiable functions, in *2020 IEEE International Conference on Quantum Computing and Engineering (QCE)* (IEEE, 2020), pp. 169–179.

[21] S. Wang, E. Fontana, M. Cerezo, K. Sharma, A. Sone, L. Cincio, and P. J. Coles, Noise-induced barren plateaus in variational quantum algorithms, Nat. Commun. **12**, 6961 (2021).

[22] M. Larocca, S. Thanasilp, S. Wang, K. Sharma, J. Biamonte, P. J. Coles, L. Cincio, J. R. McClean, Z. Holmes, and M. Cerezo, A review of barren plateaus in variational quantum computing, Nat. Rev. Phys. **7**, 174 (2025).

[23] M. Erhard, M. Krenn, and A. Zeilinger, Advances in high-dimensional quantum entanglement, Nat. Rev. Phys. **2**, 365 (2020).

[24] D. Girolami, How difficult is it to prepare a quantum state?, Phys. Rev. Lett. **122**, 010505 (2019).

[25] D. Leibfried, D. M. Meekhof, B. E. King, C. H. Monroe, W. M. Itano, and D. J. Wineland, Experimental determination of the motional quantum state of a trapped atom, Phys. Rev. Lett. **77**, 4281 (1996).

[26] M. Hofheinz, H. Wang, M. Ansmann, R. C. Bialczak, E. Lucero, M. Neeley, A. D. O'connell, D. Sank, J. Wenner, J. M. Martinis *et al.*, Synthesizing arbitrary quantum states in a superconducting resonator, Nature (London) **459**, 546 (2009).

[27] B. E. Anderson, H. Sosa-Martinez, C. A. Riofrío, I. H. Deutsch, and P. S. Jessen, Accurate and robust unitary transformations of a high-dimensional quantum system, Phys. Rev. Lett. **114**, 240401 (2015).

[28] X. Tan, D.-W. Zhang, W. Zheng, X. Yang, S. Song, Z. Han, Y. Dong, Z. Wang, D. Lan, H. Yan *et al.*, Experimental observation of tensor monopoles with a superconducting qudit, Phys. Rev. Lett. **126**, 017702 (2021).

[29] E. A. Wollack, A. Y. Cleland, R. G. Gruenke, Z. Wang, P. Arrangoiz-Arriola, and A. H. Safavi-Naeini, Quantum state preparation and tomography of entangled mechanical resonators, Nature (London) **604**, 463 (2022).

[30] S. P. Walborn, D. S. Lemelle, M. P. Almeida, and P. H. S. Ribeiro, Quantum key distribution with higher-order alphabets using spatially encoded qudits, Phys. Rev. Lett. **96**, 090501 (2006).

[31] A. C. Dada, J. Leach, G. S. Buller, M. J. Padgett, and E. Andersson, Experimental high-dimensional two-photon entanglement and violations of generalized bell inequalities, Nat. Phys. **7**, 677 (2011).

[32] Y. Chu, P. Kharel, T. Yoon, L. Frunzio, P. T. Rakich, and R. J. Schoelkopf, Creation and control of multi-phonon fock states in a bulk acoustic-wave resonator, Nature (London) **563**, 666 (2018).

[33] S. E. Venegas-Andraca, Quantum walks: A comprehensive review, Quantum Info. Proc. **11**, 1015 (2012).

[34] Y. Aharonov, L. Davidovich, and N. Zagury, Quantum random walks, Phys. Rev. A **48**, 1687 (1993).

[35] A. Ambainis, E. Bach, A. Nayak, A. Vishwanath, and J. Watrous, One-dimensional quantum walks, in *Proceedings of the thirty-third annual ACM symposium on Theory of computing* (ACM, New York, 2001), pp. 37–49.

[36] P. Ribeiro, P. Milman, and R. Mosseri, Aperiodic quantum random walks, Phys. Rev. Lett. **93**, 190503 (2004).

[37] M. C. Bañuls, C. Navarrete, A. Pérez, E. Roldán, and J. C. Soriano, Quantum walk with a time-dependent coin, Phys. Rev. A **73**, 062304 (2006).

[38] M. Montero, Invariance in quantum walks with time-dependent coin operators, Phys. Rev. A **90**, 062312 (2014).

[39] D. Bulger, J. Freckleton, and J. Twamley, Position-dependent and cooperative quantum parrondo walks, New J. Phys. **10**, 093014 (2008).

[40] Y. Shikano and H. Katsura, Localization and fractality in inhomogeneous quantum walks with self-duality, Phys. Rev. E **82**, 031122 (2010).

[41] P. Xue, H. Qin, B. Tang, and B. C. Sanders, Observation of quasiperiodic dynamics in a one-dimensional quantum walk of single photons in space, New J. Phys. **16**, 053009 (2014).

[42] A. P. Flitney, D. Abbott, and N. F. Johnson, Quantum walks with history dependence, J. Phys. A: Math. Gen. **37**, 7581 (2004).

[43] P. P. Rohde, G. K. Brennen, and A. Gilchrist, Quantum walks with memory provided by recycled coins and a memory of the coin-flip history, Phys. Rev. A **87**, 052302 (2013).

[44] A. Joye and M. Merkli, Dynamical localization of quantum walks in random environments, J. Stat. Phys. **140**, 1025 (2010).

[45] A. Joye, Random time-dependent quantum walks, Commun. Math. Phys. **307**, 65 (2011).

[46] R. Vieira, E. P. M. Amorim, and G. Rigolin, Dynamically disordered quantum walk as a maximal entanglement generator, Phys. Rev. Lett. **111**, 180503 (2013).

[47] G. Di Molfetta, D. O. Soares-Pinto, and S. M. Duarte Queirós, Elephant quantum walk, Phys. Rev. A **97**, 062112 (2018).

[48] M. A. Pires, G. Di Molfetta, and S. M. Duarte Queirós, Multiple transitions between normal and hyperballistic diffusion in quantum walks with time-dependent jumps, Sci. Rep. **9**, 19292 (2019).

[49] L. Grover and T. Rudolph, Creating superpositions that correspond to efficiently integrable probability distributions, arXiv:quant-ph/0208112.

[50] M. Montero, Quantum and random walks as universal generators of probability distributions, Phys. Rev. A **95**, 062326 (2017).

[51] R. Zhang, R. Yang, J. Guo, C.-W. Sun, Y.-C. Liu, H. Zhou, P. Xu, Z. Xie, Y.-X. Gong, and S.-N. Zhu, Arbitrary coherent distributions in a programmable quantum walk, Phys. Rev. Res. **4**, 023042 (2022).

[52] J. Wang and K. Manouchehri, *Physical Implementation of Quantum Walks* (Springer, Heidelberg, 2013).

[53] X. Qiang, Y. Wang, S. Xue, R. Ge, L. Chen, Y. Liu, A. Huang, X. Fu, P. Xu, T. Yi *et al.*, Implementing graph-theoretic quantum algorithms on a silicon photonic quantum walk processor, Sci. Adv. **7**, eabb8375 (2021).

[54] H. Tang, X.-F. Lin, Z. Feng, J.-Y. Chen, J. Gao, K. Sun, C.-Y. Wang, P.-C. Lai, X.-Y. Xu, Y. Wang *et al.*, Experimental two-dimensional quantum walk on a photonic chip, Sci. Adv. **4**, eaat3174 (2018).

[55] M. Karski, L. Förster, J.-M. Choi, A. Steffen, W. Alt, D. Meschede, and A. Widera, Quantum walk in position space with single optically trapped atoms, Science **325**, 174 (2009).

[56] J. Carlström, N. Prokof'ev, and B. Svistunov, Quantum walk in degenerate spin environments, Phys. Rev. Lett. **116**, 247202 (2016).

[57] M. Gong, S. Wang, C. Zha, M.-C. Chen, H.-L. Huang, Y. Wu, Q. Zhu, Y. Zhao, S. Li, S. Guo *et al.*, Quantum walks on a programmable two-dimensional 62-qubit superconducting processor, Science **372**, 948 (2021).

[58] E. Flurin, V. V. Ramasesh, S. Hacohen-Gourgy, L. S. Martin, N. Y. Yao, and I. Siddiqi, Observing topological invariants using

quantum walks in superconducting circuits, Phys. Rev. X **7**, 031023 (2017).

[59] W.-W. Zhang, S. K. Goyal, F. Gao, B. C. Sanders, and C. Simon, Creating cat states in one-dimensional quantum walks using delocalized initial states, New J. Phys. **18**, 093025 (2016).

[60] C. M. Chandrashekar, R. Srikanth, and R. Laflamme, Optimizing the discrete time quantum walk using a SU(2) coin, Phys. Rev. A **77**, 032326 (2008).

[61] H. Majury, J. Boutari, E. O'Sullivan, A. Ferraro, and M. Paternostro, Robust quantum state engineering through coherent localization in biased-coin quantum walks, EPJ Quantum Tech. **5**, 1 (2018).

[62] A. Gratsea, M. Lewenstein, and A. Dauphin, Generation of hybrid maximally entangled states in a one-dimensional quantum walk, Quantum Sci. Technol. **5**, 025002 (2020).

[63] L. Innocenti, H. Majury, T. Giordani, N. Spagnolo, F. Sciarrino, M. Paternostro, and A. Ferraro, Quantum state engineering using one-dimensional discrete-time quantum walks, Phys. Rev. A **96**, 062326 (2017).

[64] T. Giordani, E. Polino, S. Emiliani, A. Suprano, L. Innocenti, H. Majury, L. Marrucci, M. Paternostro, A. Ferraro, N. Spagnolo *et al.*, Experimental engineering of arbitrary qudit states with discrete-time quantum walks, Phys. Rev. Lett. **122**, 020503 (2019).

[65] J. Nie, M. Li, and X. Sun, Multipartite high-dimensional quantum state engineering via discrete-time quantum walk, Phys. Rev. A **109**, 032229 (2024).

[66] C. Esposito, F. Di Colandrea, F. Hoch, G. Carvacho, F. Cardano, N. Spagnolo, L. Marrucci, and F. Sciarrino, Generation of high-dimensional qudit quantum states via two-dimensional quantum walks, Phys. Rev. Res. **5**, 043025 (2023).

[67] P. Kurzyński and A. Wójcik, Quantum walk as a generalized measuring device, Phys. Rev. Lett. **110**, 200404 (2013).

[68] Y.-Y Zhao, N.-K Yu, P. Kurzyński, G.-Y Xiang, C.-F. Li, and G.-C. Guo, Experimental realization of generalized qubit measurements based on quantum walks, Phys. Rev. A **91**, 042101 (2015).

[69] X. Wang, X. Zhan, Y. Li, L. Xiao, G. Zhu, D. Qu, Q. Lin, Y. Yu, and P. Xue, Generalized quantum measurements on a higher-dimensional system via quantum walks, Phys. Rev. Lett. **131**, 150803 (2023).

[70] N. Inui, N. Konno, and E. Segawa, One-dimensional three-state quantum walk, Phys. Rev. E **72**, 056112 (2005).

[71] Y. Wang, H. Jiang, Y. Liu, and K. Li, Direct measurement of density matrices via dense dual bases, arXiv:2409.03435.

[72] N. Konno, Quantum random walks in one dimension, Quantum Info. Proc. **1**, 345 (2002).

[73] N. Konno, T. Namiki, and T. Soshi, Symmetry of distribution for the one-dimensional hadamard walk, Interdiscip. Inf. Sci. **10**, 11 (2004).

[74] A. Ambainis, J. Kempe, and A. Rivosh, Coins make quantum walks faster, arXiv:quant-ph/0402107.